Far-infrared laser vibration–rotation–tunneling spectroscopy of the propane–water complex: Torsional dynamics of the hydrogen bond

David W. Steyert,[a] Matthew J. Elrod, and Richard J. Saykally
Department of Chemistry, University of California, Berkeley, California 94720

(Received 17 March 1993; accepted 3 August 1993)

The far-infrared laser vibration–rotation–tunneling (FIR-VRT) spectrum of the propane–water complex has been measured in the range 18–22 cm^{-1}. A *C*-type VRT band has been assigned with a band origin of 19.6 cm^{-1}. The data support the "kite-shaped" structure determined from microwave spectroscopy in the accompanying paper, and indicate that the observed VRT band corresponds to torsional motion of the free water proton about the hydrogen bond. This motion is impeded by a barrier that is less than 5 cm^{-1}. We describe our modification of the supersonic slit-jet source designed to permit Stark effects to be measured, and have used second-order Stark shifts to help assign the perpendicular transition observed.

I. INTRODUCTION

The "hydrophobic effect" is of central importance in chemistry and biology. While there is a general agreement that the effect is principally a result of disrupting the strong hydrogen bonding networks in the aqueous phase, controversy exists with respect to molecular descriptions of the phenomenon.[1–5] This controversy is principally due to the lack of accurate intermolecular potential surfaces (IPS) for describing the interactions between water and even simple hydrophobes, as well as suitable analytical forms for describing these surfaces in dynamical calculations.

The simplest class of water–hydrophobe systems are comprised of water interacting with the rare gases. We have recently completed an extensive study[6–10] of the prototypical H_2O–Ar cluster which has culminated in the determination of a very detailed three-dimensional intermolecular pair potential surface[8,10] (IPS), obtained by direct inversion of far-infrared vibration–rotation–tunneling (FIR-VRT) spectra. This new and accurate IPS could be employed for improved simulations of hydrophobic hydration, as previously carried out by several groups using only a crude guess for this crucial property. The hydrophobic effect will depend principally on the short-range portion of the solute-water IPS, as this forces the hydrogen bonding rearrangement in the solvent. Our new IPS (AW2)[10] exhibits a more complicated topology in its repulsive wall that was not inherent in the simple pair potential used in the simulations.

The next level of complexity that we have investigated is water interacting with the simplest saturated hydrocarbon-methane.[11,12] This system constitutes a significant escalation in the VRT dynamics, since these are now described by *six* large amplitude coordinates, rather than the three dimensions that characterize atom–polyatom interactions. Accordingly, the current IPS for this system is of necessity, a more primitive one, although it does appear to possess the correct qualitative features.

In the present paper and in its counterpart,[13] we present our results for the water–propane complex. We have chosen this system as the third level of complexity because it is the simplest that allows us to address the interactions between water and both a methyl and methylene group. We note that the recent work of Blake and co-workers[14] has addressed the important subject of water–aromatic interactions in the same fashion, viz. by a combined microwave FIR-VRT spectroscopy approach.

II. EXPERIMENT

The Berkeley tunable far-infrared spectrometer has been described in detail previously,[15] so only a brief discussion of the technique and the modifications incorporated to permit measurements of the Stark effect will be presented here. Fixed-frequency far-infrared radiation is generated by continuously pumping a 3-m molecular gas far-infrared laser with a 100 W CO_2 laser. To provide continuously tunable FIR radiation, the fixed-frequency FIR laser output is optically coupled onto a gold-nickel antenna (0.2 mm–1 mm long) which acts as one lead of a GaAs Schottky-barrier diode. By also applying tunable microwave radiation (2–110 GHz) to this diode, sum and difference frequencies are generated by nonlinear mixing in the diode, and these are then reradiated by the antenna. A Martin–Puplett polarizing diplexer interferometrically separates these sidebands from the much stronger fixed-frequency laser signal.

After leaving the diplexer, both sidebands are directed to a multipass cell similar to that described by Kaur and co-workers.[16,17] This provides several (typically 10) passes of the laser in front of a planar supersonic jet, a 10 cm long continuous nozzle with a spacing between jaws of slightly over 25 μm.[15,18] An absorptive loss in the sideband power is detected with either a Rollins-mode indium antimonide detector or a Putley-mode indium antimonide detector. Lock-in detection was used with 50 kHz frequency modulation of the microwave frequency and 2-f demodulation. The expansion chamber, an 8 in. (20 cm) six-way cross, was pumped by a 2500 cfm Roots pump (Edwards

[a]Present address: Department of Chemistry and Physics, Beaver College, Glenside, PA 19038.

TABLE I. Lasers used in the spectroscopy of the propane–water complex. Frequencies are taken from Ref. 19. Sidebands from parallel lasers pass through the chamber polarized parallel to the dc electric field.

Frequency (GHz)	Wavelength (μm)	Lasing gas	Polarization	Pump
527.9260	568	DCOOD	Parallel	10R26
584.3882	513	HCOOH	Parallel	9R28
639.1846	469	CH_3OH	Perpendicular	10R38
692.9513	432	HCOOH	Parallel	9R20
716.1574	419	HCOOH	Parallel	9R22
761.6083	394	HCOOH	Parallel	9R18
768.8820	389	DCOOD	Parallel	10R12
787.7555	380	DCOOD	Parallel	10R12

EH4200) backed by one 255 cfm two-stage mechanical pump (Edwards E2M275), as described in Ref. 18.

Far-infrared spectra of a supersonic expansion containing 3% propane (instrument purity, 99.5%, flow rate 0.02 sscfm, Matheson) in argon (99.995% pure, Liquid Air Corporation) at 7 psi (gauge) (1120 Torr) and saturated with distilled water were recorded in the frequency range from 498 to 810 GHz (16.6–27.0 cm^{-1}). If either sideband was near a water absorption, the entire beam path was sealed and purged with dry nitrogen.

The far-infrared lasing transitions used are listed in Table I. Frequencies are taken from Ref. 19. One of the strongest FIR transitions is shown in Fig. 1. The observed signal-to-noise ratio ranged from 1:1 to 35:1.

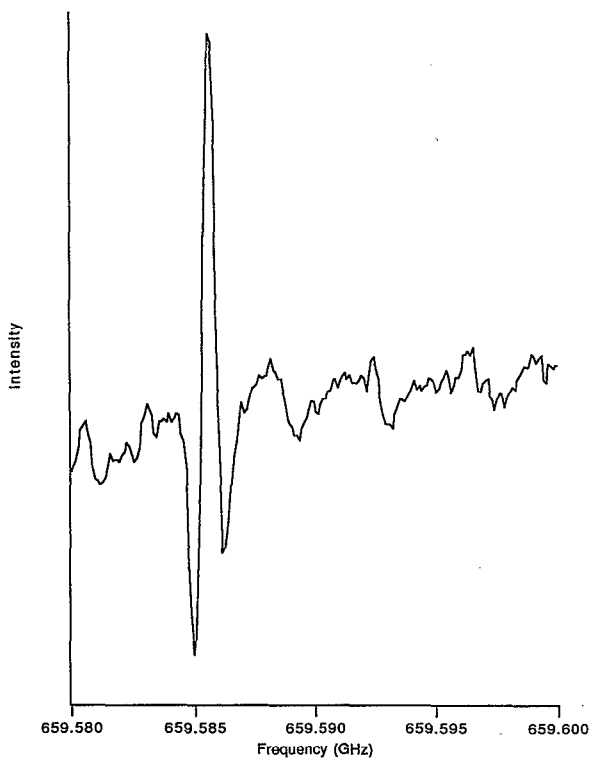

FIG. 1. One of the strongest FIR absorptions ($5_{50} \leftarrow 4_{40}$) measured in the spectrum of the propane–water complex.

To assist in assigning the complicated spectrum observed for the propane–water complex, the Stark effect was used. The use of a dc electric field as an assignment tool in microwave spectroscopy is well known,[20] and has additionally been used in intracavity far-infrared spectroscopy by Ray *et al.*[21] and in the molecular beam electric resonance (MBER) technique of Marshall *et al.*[22] However, this represents the first application of Stark spectroscopy with tunable FIR lasers, or with planar supersonic jets.

The most practical way to apply a Stark field to the slit-jet source in the FIR spectrometer is parallel to the face of the slit jet. The polarization of the FIR laser for most of the lasing transitions used in this study thereby results in the Stark field being applied parallel to the electric field of the laser. Using another Stark field geometry described below permits at least some control over this relative polarization. Two 3 mm thick aluminum plates, each 12.7 cm long by 15.2 cm wide, were hand polished to achieve uniform flatness. The Stark plates are supported above and below the slit jet body, which is 11.4 cm long and 2.54 cm high, and are spaced from it by 2.5 cm Plexiglas blocks. This yields a 7.6 cm plate spacing. Of the 12.7 cm of Stark plate length, only 10.1 cm project beyond the face of the slit. Two Plexiglas rods run beside the slit source, and attach the Plexiglas blocks to each other, sandwiching the stainless steel source between them. Equal and opposite electric potentials are applied to the two plates relative to the source, which is grounded. There is also a voltmeter outside the chamber to measure the actual potential across the plates.

Additional experiments were attempted in which the Stark field was applied between the slit jet and a parallel horizontal wire in front of it. Because this geometry was more difficult to align, and was therefore less reproducible, this approach was abandoned. In spite of this disadvantage, this does permit the generation of a Stark field perpendicular to that applied by the parallel-plate geometry described earlier.

Fortunately, the presence of the Stark plates did not substantially intefere with the supersonic expansion dynamics (thus heating the beam) and the electric fields obtained were sufficiently uniform to permit narrow linewidths to be observed. The upper limit on the Stark field that can be applied is determined by the dielectric breakdown voltage of the gas between them. In an argon expansion, with our geometry, this limits the potential to 340 V. Across the 7.6 cm spacing, this is 44.6 V/cm. With zero-field linewidths of about 1 MHz, this is adequate for observing most first-order Stark splittings and for fast tuning second-order splittings. A representative spectrum appears in Fig. 2.

III. EXPERIMENTAL RESULTS AND DISCUSSION

Spectral lines were measured in the frequency range from 503 to 713 GHz, a range of 7 cm^{-1}. Of the over 600 lines initially observed, 154 lines of the complicated ($\kappa = -0.85$), spectrum observed were eventually assigned to *C*-type vibrational transition originating from the *ortho* ground state identified in the accompanying paper.

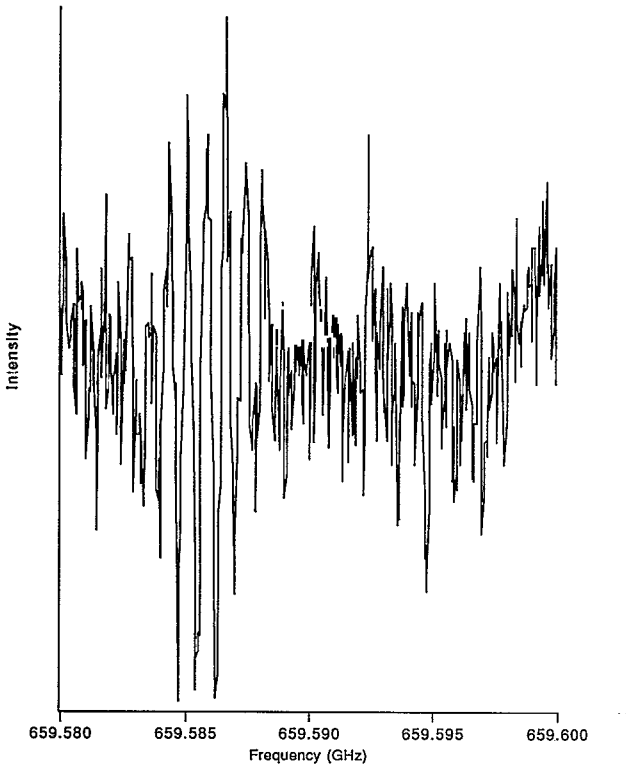

FIG. 2. One of the more well-resolved Stark spectra of the propane–water complex. This is the $5_{50} \leftarrow 4_{40}$ transition depicted at zero field in Fig. 1. In this spectrum, the Stark field was applied horizontally, parallel to the laser polarization.

The technique of common-upper-state combination differences was used to assign this spectrum, using and refining the lower-state constants presented in the previous paper. However, some pairs of transitions assigned by combination differences were at energies incompatible with the upper-state constants. This indicated that some upper rotational levels were affected by a strong resonant-type mixing, so the fitting was performed by combining FIR combination differences with microwave data assigned an uncertainty of 1.5 MHz to the combination differences and an uncertainty of 0.004 MHz to the microwave transitions. The ground-state constants determined in this fit are presented in Table II. With the ground-state constants fixed at the values so obtained, the upper state can be characterized by a direct fit of the far-infrared spectrum, assigning an uncertainty of 1 MHz to each individual transition. The resulting Watson *S*-reduced constants[23] are also shown in Table II, and the assignment and residuals of the upper-state fit are shown in Table III. The resulting fit is within the estimated experimental uncertainty, with a standard deviation of 1.1 MHz.

Experiments with the Stark plates described above yielded some important information for assigning the propane–water spectrum. All the far-infrared absorptions between 558 and 702 GHz were checked for a Stark effect, initially by using the background-subtract feature of the data acquisition program to subtract a 25 MHz scan with the gas on, but the Stark fields off, from the previous scan

TABLE II. Watson *S*-reduced constants from the far-infrared and microwave spectra of *ortho* propane–water via a weighted least-squares fit. The sum-of-squares deviation is 1.1 MHz. Uncertainties are one standard deviation in the last digits.

Lower state			Upper state		
			ν_0	579 691.20(24)	MHz
A	8443.24(12)	MHz	A	8512.765(61)	MHz
B	2507.6611(22)	MHz	B	2503.631(18)	MHz
C	1969.3165(22)	MHz	C	1997.940(18)	MHz
D_J	0.010 203(78)	MHz	D_J	0.012 009(61)	MHz
D_{JK}	0.211 44(50)	MHz	D_{JK}	0.0870(12)	MHz
D_K	0.0[a]	MHz	D_K	0.0510(28)	MHz
d_1	0.004 166(46)	MHz	d_1	0.003 348(94)	MHz
d_2	0.008 68(49)	MHz	d_2	−0.000 875(29)	MHz
H_J	0.000 002 3(18)	MHz	H_J	0.0[a]	MHz
H_{JK}	0.000 009 5(23)	MHz	H_{JK}	−0.000 021 6(74)	MHz
H_{KJ}	−0.001 26(12)	MHz	H_{KJ}	−0.000 027(25)	MHz
H_K	−0.0151(22)	MHz	H_K	−0.010 539(25)	MHz

[a]Value within one standard deviation of zero, fixed at zero for this fit.

taken with the Stark fields set on the highest field accessible: 320–340 V. Transitions showing a frequency shift, such as that due to a second-order Stark effect, would appear with a "third-derivative" line shape because of our initial 2-f detection scheme.

This Stark shift scanning approach indicated pairs of lines of nearly equal intensities that Stark-shifted toward or away from each other. Some of those pairs that shifted toward each other also fell in linear-rotor patterns with a spacing of about 4.65 GHz. All lines that showed Stark shifts, along with their eventual assignment, are shown in Table IV. Several of these lines were assigned as the two components of a slightly split asymmetry doublet, consistent with the pseudo-first-order Stark shifts expected for nearly degenerate states.

IV. DISCUSSION

By analogy to ArH_2O,[10] one possible interpretation of this band would be that of a H_2O internal rotation transition (i.e., the $1_{10} \leftarrow 1_{01}$ transition of free water, which occurs at 18.5 cm^{-1}) involving the lowest two rotational states of *ortho* water. If the propane exerts only a weak force on the water, then the internal rotor transition in the complex will be relatively unchanged from this frequency. This model also predicts that the permanent dipole of the complex would be near zero, for there would be little net orientation of the water within the complex. Therefore, one possible assignment would be that of an ArH_2O-like $1_{10}\,\Pi \leftarrow 1_{01}\,\Sigma$ water internal rotor transition, with the Π state split by the asymmetry of the propane subunit into an in-plane and out-of-plane vibration (transitions to the out-of-plane bend would follow *C*-type selection rules). This specific interpretation has been shown to apply to the Ar_2HCl system.[24]

This model would be entirely consistent: Propane–water has a very isotropic IPS such that the water molecule executes nearly free internal rotation with its dipole on average slightly aligned along the propane b axis (the complex a axis). However, a problem arises when comparing

TABLE III. The assignment and fit of the far-infrared and microwave spectra of propane–water.

	Upper state			Lower state			Observed frequency	Residual O–C
v	J	K_a	K_c	J	K_a	K_c	MHz	MHz
0	2	0	2	1	0	1	8 918.654	0.001
0	2	1	1	1	1	0	9 490.991	0.001
0	3	1	3	2	1	2	12 600.302	−0.002
0	3	0	3	2	0	2	13 290.925	−0.000
0	3	2	2	2	2	1	13 424.763	0.002
0	3	1	2	2	1	1	14 213.021	0.002
0	4	1	4	3	1	3	16 762.135	0.004
0	4	0	4	3	0	3	17 564.257	−0.003
0	4	2	3	3	2	2	17 871.446	−0.002
1	9	0	9	10	1	9	512 430.5	−0.831
1	8	0	8	9	1	8	519 975.6	−0.295
1	6	0	6	7	1	6	534 301.8	0.371
1	5	0	5	6	1	5	540 918.1	−0.142
1	4	0	4	5	1	4	547 137.4	−0.685
1	3	0	3	4	1	3	552 987.8	0.635
1	2	0	2	3	1	2	558 511.6	1.431
1	1	0	1	2	1	1	563 751.9	0.906
1	0	0	0	1	1	0	568 739.7	−0.755
1	1	0	1	1	1	1	573 779.9	−0.398
1	2	0	2	2	1	2	574 337.9	−0.023
1	3	0	3	3	1	3	575 120.5	0.991
1	4	0	4	4	1	4	576 062.1	0.578
1	5	0	5	5	1	5	577 089.6	1.208
1	6	0	6	6	1	6	578 129.0	2.336
1	8	0	8	8	1	8	580 046.2	1.383
1	9	0	9	9	1	9	580 897.4	0.811
1	10	0	10	10	1	10	581 692.2	−0.121
1	1	1	0	0	0	0	590 707.0	−0.190
1	2	1	1	1	0	1	595 738.8	0.596
1	3	1	2	2	0	2	601 061.4	0.562
1	4	1	3	3	0	3	606 718.0	−0.151
1	5	1	4	4	0	4	612 772.4	1.194
1	6	1	5	5	0	5	619 285.8	1.253
1	7	1	6	6	0	6	626 303.1	−0.368
1	8	1	7	7	0	7	633 830.5	−0.524
1	9	1	8	8	0	8	641 817.5	0.043
1	10	1	9	9	0	9	650 167.8	−0.403
1	11	1	10	10	0	10	658 766.3	0.615
1	11	1	10	12	2	10	504 112.6	−1.625
1	10	1	9	11	2	9	510 520.9	−1.003
1	9	1	9	10	2	9	506 755.7	−0.881
1	9	1	8	10	2	8	516 479.6	−0.776
1	8	1	8	9	2	8	513 062.4	−0.883
1	8	1	7	8	2	7	570 361.1	−0.300
1	6	1	6	7	2	6	525 179.6	−0.220
1	6	1	5	7	2	5	531 839.2	−0.633
1	5	1	4	6	2	4	536 245.1	−0.644
1	5	1	5	6	2	5	530 954.4	−0.313
1	4	1	3	5	2	3	540 399.0	−0.678
1	3	1	2	4	2	2	544 401.8	−0.823
1	3	1	3	4	2	3	541 884.3	−0.830
1	2	1	2	3	2	2	547 028.7	−1.641
1	2	1	1	3	2	1	548 373.1	−0.238
1	1	1	1	2	2	1	551 956.9	−1.306
1	1	1	0	2	2	0	552 427.3	−1.577
1	2	1	1	2	2	1	561 972.3	0.538
1	3	1	2	3	2	2	562 788.7	0.413
1	4	1	3	4	2	3	563 866.4	1.322
1	5	1	4	5	2	4	565 190.1	1.783
1	6	1	5	6	2	5	566 736.8	0.652
1	7	1	6	7	2	6	568 476.6	0.749
1	9	1	8	9	2	8	572 334.5	1.623
1	10	1	9	10	2	9	574 320.7	0.921
1	11	1	10	11	2	10	576 250.1	0.386

TABLE III. (*Continued.*)

	Upper state			Lower state			Observed frequency	Residual O–C
v	J	K_a	K_c	J	K_a	K_c	MHz	MHz
1	14	1	13	14	2	13	581 204.8	0.765
1	11	2	10	11	1	10	587 093.8	−0.794
1	9	2	8	9	1	8	589 491.0	0.105
1	8	2	7	8	1	7	590 909.0	0.297
1	7	2	6	7	1	6	592 356.4	0.418
1	6	2	5	6	1	5	593 753.3	0.012
1	5	2	4	5	1	4	595 034.3	−2.528
1	4	2	3	4	1	3	596 161.5	2.267
1	3	2	2	3	1	2	597 087.9	0.587
1	2	2	1	2	1	1	597 798.9	−0.010
1	2	2	0	1	1	0	607 320.8	0.363
1	2	2	1	1	1	1	607 828.7	0.486
1	3	2	1	2	1	1	611 451.1	−1.135
1	3	2	2	2	1	2	612 915.9	0.833
1	4	2	2	3	1	2	615 515.9	1.267
1	4	2	3	3	1	3	618 293.1	1.524
1	5	2	3	4	1	3	619 616.7	−2.505
1	6	2	4	5	1	4	623 883.8	−1.631
1	6	2	5	5	1	5	629 921.7	−1.739
1	7	2	5	6	1	5	628 422.9	−1.627
1	7	2	6	6	1	6	636 180.0	−1.217
1	8	2	6	7	1	6	633 328.1	−1.811
1	8	2	7	7	1	7	624 728.9	−0.831
1	9	2	8	8	1	8	649 559.1	−0.717
1	10	2	8	9	1	8	644 531.9	−2.330
1	10	2	9	9	1	9	656 655.0	−1.511
1	11	2	9	10	1	9	650 954.4	1.179
1	11	2	10	10	1	10	663 999.6	0.144
1	12	2	10	11	1	10	657 970.4	0.023
1	7	2	6	8	3	6	512 635.8	1.854
1	11	3	9	11	2	9	602 224.3	1.411
1	10	3	8	10	2	8	604 285.9	0.974
1	7	3	5	7	2	5	609 077.0	1.332
1	6	3	4	6	2	4	610 046.8	−0.035
1	4	3	2	4	2	2	611 054.3	−0.966
1	3	3	1	3	2	1	611 213.8	1.255
1	3	3	0	2	2	0	624 778.6	1.412
1	3	3	1	2	2	1	624 812.3	1.332
1	4	3	1	3	2	1	629 272.9	−2.412
1	4	3	2	3	2	2	629 438.8	−2.130
1	7	3	4	6	2	4	641 951.6	−0.330
1	7	3	5	6	2	5	643 972.7	0.716
1	8	3	5	7	2	5	645 795.1	0.221
1	8	3	6	7	2	6	649 139.4	1.887
1	9	3	6	8	2	6	649 503.4	−0.116
1	10	3	7	9	2	7	653 190.3	1.716
1	10	3	8	9	2	8	660 138.0	0.573
1	11	3	8	10	2	8	656 989.0	−1.201
1	11	3	9	10	2	9	666 020.2	−0.565
1	12	3	10	11	2	10	672 181.0	−1.319
1	13	3	11	12	2	11	678 629.7	−0.393
1	4	4	1	4	3	1	624 179.1	0.833
1	5	4	2	5	3	2	624 238.1	−0.252
1	8	4	5	8	3	5	624 023.4	0.092
1	9	4	6	9	3	6	623 639.9	1.148
1	10	4	7	10	3	7	622 980.4	2.448
1	4	4	0	3	3	0	642 141.6	−0.526
1	4	4	1	3	3	1	642 143.0	−0.507
1	5	4	1	4	3	1	646 732.7	−1.503
1	5	4	2	4	3	2	646 742.3	−1.475
1	7	4	3	6	3	3	655 891.2	−0.437
1	7	4	4	6	3	4	656 002.8	−0.125
1	8	4	4	7	3	4	660 400.7	1.731
1	8	4	5	7	3	5	660 671.8	1.388

TABLE III. (*Continued.*)

	Upper state			Lower state			Observed frequency	Residual O–C
v	J	K_a	K_c	J	K_a	K_c	MHz	MHz
1	9	4	6	8	3	6	665 380.6	1.942
1	10	4	7	9	3	7	670 147.8	0.136
1	11	4	7	10	3	7	673 074.5	1.952
1	5	5	0	4	4	0	659 585.7	0.550
1	6	5	1	5	4	1	664 212.5	0.048
1	7	5	2	6	4	2	668 856.0	1.892
1	7	5	3	6	4	3	668 858.0	1.829
1	8	5	3	7	4	3	673 501.3	−1.415
1	8	5	4	7	4	4	673 508.8	−1.400
1	9	5	4	8	4	4	678 146.0	−2.029
1	9	5	5	8	4	5	678 168.1	−2.088
1	11	5	6	10	4	6	687 366.0	0.148
1	9	6	4	9	5	4	650 750.2	−1.017
1	10	6	5	10	5	5	650 925.9	−2.327
1	11	6	6	11	5	6	651 092.7	−0.074
1	6	6	0	5	5	0	677 096.1	0.477
1	6	6	1	6	5	1	650 225.1	−0.504
1	9	6	3	8	5	3	691 140.3	−0.758
1	10	6	4	9	5	4	695 845.9	−0.607
1	10	6	5	9	5	5	695 847.2	−0.683
1	11	6	5	10	5	5	700 553.3	−0.334
1	11	6	6	10	5	6	700 557.4	−0.320
1	10	7	4	10	6	4	664 067.7	1.277
1	8	7	2	7	6	2	699 362.3	1.576
1	11	7	4	10	6	4	713 613.3	0.891
1	8	8	1	7	7	1	712 219.5	−1.259

this with the data available for the methane–water complex.[12] The water–methane complex has been shown to have a dipole moment large enough such that pure rotational transitions are easily observed.[12] In terms of electrostatic forces, propane differs from methane in that it possesses low order nonzero permanent moments: an appreciable quadrupole, and a dipole that is small but finite, 0.083 D.[25] This argument indicates that propane–water should be more rigidly bound than methane–water, and consequently that it would have a larger dipole moment in its ground state. However, the contributions of the repulsive interactions to the overall anisotropy are not easy to assess in an *a priori* fashion, and these may actually be the determining factors in establishing the effective rigidity of the two complexes.

In the discussion which follows, it will be helpful to introduce some elements of group theory. The microwave spectrum of free propane is characterized by a small tunneling splitting of between 100 and 600 kHz,[25] representing the hindered internal rotation of the two methyl subunits relative to the whole. The well depth parameter, (V_3), is 1108 (± 10) cm^{-1}. There is also a slight top–top coupling, (V'_{12}), of $-51.8(\pm 8)$ cm^{-1}.[25] The resulting sublevels are labeled AA, AE, EA, and EE, according to the symmetry of the individual wave function for each methyl group. For pure rotational transitions, the selection rules are given by

$$\text{AA}\leftrightarrow\text{AA} \quad \text{AE}\leftrightarrow\text{AE} \quad \text{EA}\leftrightarrow\text{EA} \quad \text{EE}\leftrightarrow\text{EE}. \qquad (1)$$

In discussing the far-infrared spectrum of the propane–water complex, the situation is further simplified. The tunneling splittings due to methyl group torsion observed in high-resolution microwave experiments are small compared to the accuracy and linewidth of the far-infrared spectrometer. If one could observe the spectrum of uncomplexed propane with the far-infrared spectrometer, the torsions would therefore introduce unmeasurable tunneling splittings, so that they are, for the purposes of the far-infrared spectrum of propane, chemically unfeasible, in the sense described by Bunker.[26]

As a result, the group theory of the propane–water complex can be considerably simplified by labeling the two equivalent methyl groups, 1 and 2, and the two protons of the water A and B. Both the C_{2v} and hydrogen-bonded equivalent frameworks are shown in Fig. 3. In the following, we explicitly discuss the hydrogen-bonded reference geometry for reasons which will become clear. In discussing the symmetry considerations for an assignment of the far-infrared transition, it is important to distinguish between two tunneling paths shown in the lower portion of Fig. 3. The tunneling path $1\rightarrow 2$, which interchanges the water hydrogen atoms, introduces the nuclear spin selection rules appropriate to the water monomer, while the tunneling path $1\rightarrow 3$ is governed by the much relaxed selection rules of the two methyl groups. Since each rotational level has methyl-group tunneling components of all symmetries, the nuclear spin of the propane hydrogen atoms will not be a factor in establishing the VRT selection rules.

To get a first estimate of the potential for rotation of

TABLE IV. Assigned far-infrared absorption frequencies (GHz) showing resolvable Stark shifts for $E \simeq 40$ V/cm. The pairs of asymmetry doublets are readily apparent. The second column lists the direction of the shift: b=to higher frequency, r=to lower frequency, s=split slightly.

		Upper state			Lower state		
Frequency	Shift	J	K_a	K_c	J	K_a	K_c
561.9723	b	2	1	1	2	2	1
562.7887	b	3	1	2	3	2	2
565.1901	r	5	1	4	5	2	4
576.2501	r	11	1	10	11	2	10
563.7519	r	1	0	1	2	1	1
573.7799	b	1	0	1	1	1	1
577.0896	r	5	0	5	5	1	5
580.8974	b	9	0	9	9	1	9
581.6922	r	10	0	10	10	1	10
597.0879	r	3	2	2	3	1	2
597.7989	r	2	2	1	2	1	1
607.8287	r	2	2	1	1	1	1
611.4528	b	3	2	1	2	1	1
612.9159	r	3	2	2	2	1	2
619.6167	r	5	2	3	4	1	3
636.1800	b	7	2	6	6	1	6
633.3281	b	8	2	6	7	1	6
650.9544	s	11	2	9	10	1	9
590.7070	b	1	1	0	0	0	0
601.0614	b	3	1	2	2	0	2
619.2858	r	6	1	5	5	0	5
650.1678	r	10	1	9	9	0	9
602.2243	r	11	3	9	11	2	9
610.0468	r	6	3	4	6	2	4
611.0543	r	4	3	2	4	2	2
624.7786	s	3	3	0	2	2	0
624.8123	s	3	3	1	2	2	1
629.2729	r	4	3	1	3	2	1
629.4388	s	4	3	2	3	2	2
634.1520	r	5	3	3	4	2	3
651.3104	b	10	3	7	9	2	7
656.9890	r	11	3	8	10	2	8
610.6872	r	5	3	2	5	4	2
624.0234	r	8	4	5	8	3	5
624.2381	s	5	4	2	5	3	2
624.2487	r	6	4	3	6	3	3
642.1416	b	4	4	0	3	3	0
642.1430	r	4	4	1	3	3	1
646.7327	b	5	4	1	4	3	1
646.7423	r	5	4	2	4	3	2
651.3497	s	6	4	3	5	3	3
655.8912	b	7	4	3	6	3	3
660.4007	b	8	4	4	7	3	4
665.3806	r	9	4	6	8	3	6
673.0745	b	11	4	7	10	3	7
664.2125	s	6	5	1	5	4	1
668.8560	r	7	5	2	6	4	2
668.8580	r	7	5	3	6	4	3
673.5013	b	8	5	3	7	4	3
673.5088	r	8	5	4	7	4	4
678.1460	b	9	5	4	8	4	4
678.1681	r	9	5	5	8	4	5
687.3660	b	11	5	6	10	4	6

the water subunit in the propane–water complex, a simple hindered-internal-rotor model was invoked. In this model, the wave function for the proton not involved in the hydrogen bond is a linear combination of free rotation wave functions of the form

$$\psi = (2\pi)^{-1/2} e^{\pm im\phi}, \tag{2}$$

with energies

$$\langle m | \mathscr{H} | m \rangle = Dm^2, \tag{3}$$

where D is the reciprocal of the effective moment of inertia

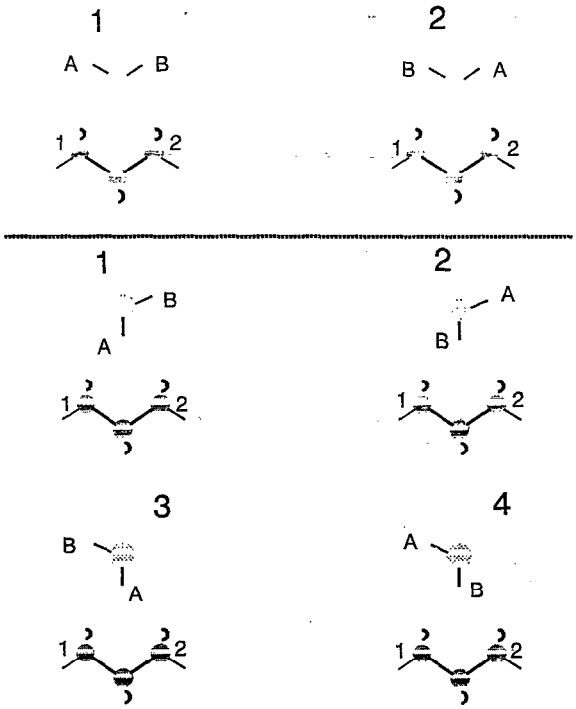

FIG. 3. The frameworks for the C_{2v} (upper) and hydrogen-bonded (lower) propane–water structures. The large numbers indicate the possible frameworks, and the small numbers and letters indicate the symmetrically equivalent components (hydrogens and methyl groups taken as a whole) of the complex.

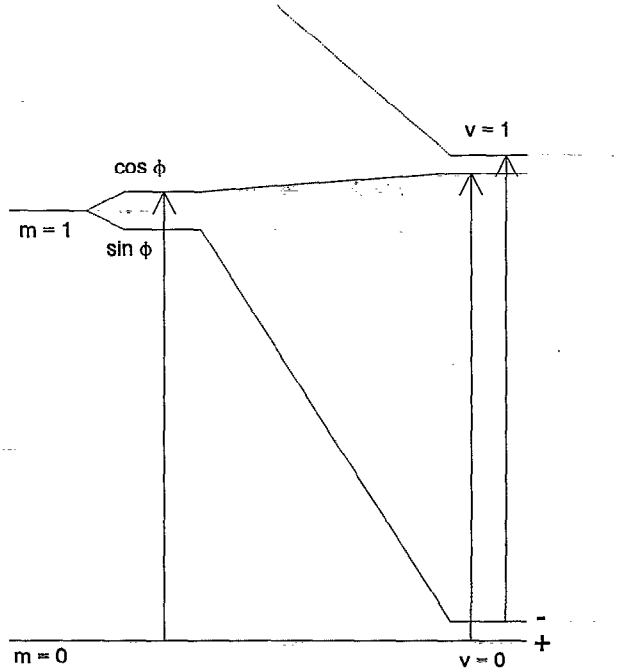

FIG. 4. A correlation diagram for the torsional motion of propane–water. On the left are the energy levels for unhindered motion ($V_2=0$) and on the right the energies in the high-barrier case. *C*-type transitions are shown with arrows.

for rotation of the subunit about the hydrogen bond, and ϕ is the torsion angle about the hydrogen bond. The potential of the problem is introduced with a term

$$V_2=\cos 2\phi \tag{4}$$

which appears in the Hamiltonian as

$$\langle m|\mathscr{H}|m\pm 2\rangle=1/2V_2. \tag{5}$$

This matrix can be diagonalized for $|m|\leqslant 8$ to yield the first few eigenvalues to an adequate level of convergence.

Stark measurements in the microwave spectrum[13] established the presence of a small *b* dipole (in the heavy-atom plane), and the complex is taken to have an equilibrium geometry in which all three water atoms are coplanar with the three carbons of propane. As a consequence, the maximum of energy must lie out of that *a*–*b* plane. Since $\phi=0$ is a maximum in $\cos 2\phi$, the zero of ϕ must be along the *c* (out-of-plane) axis. The wave function of the ground state is, to first order, symmetric about the *a* axis, but increasing the barrier V_2 concentrates the wave function in the molecular plane. The first two excited states have the wave functions

$$\Psi_s=\sin\phi, \quad \Psi_c=\cos\phi, \tag{6}$$

respectively, so that the lower energy state, Ψ_s, has its maximum probability density in the *a*–*b* molecular plane, and a node perpendicular to that plane. The transition to Ψ_s would be polarized in the molecular plane, perpendicular to the rotation (*a*) axis and therefore would be *b* polarized. Hence the state observed in this study must be the next higher one, Ψ_c (in order to match the observed *C*-type selection rules).

In the limit of a very high barrier, Ψ_s correlates to the upper tunneling states of the ground vibrational state, and the first vibrational state is doubled by the introduction of one of the states correlating to $m=\pm 2$. This is the splitting introduced by the $1\rightarrow 3$ tunneling shown in Fig. 3. There is in addition the *ortho–para* ($1\rightarrow 2$) splitting of the water. These considerations lead to the correlation scheme for the $1\rightarrow 3$ torsional motion is shown in Fig. 4.

Figure 4 shows that a *c*-type transition would be observed no matter where on the correlation diagram propane–water is, and that if it were in the high-barrier limit, there would be two *c*-type transitions in the far-infrared separated by a small tunneling splitting, and originating in different nuclear spin confirmations. In the high-barrier limit, however, both ground-state tunneling states would be thermally populated, and a total of four states would have been observed in the microwave spectrum, two from the *ortho* configuration, and two from the *para* configuration. Since this is not observed,[13] the ground-state tunneling splittings would have to be large compared to kT_{vib}, and although the rotational temperature in the NIST supersonic beam is about 1 K, this information does establish that propane–water cannot be on the high-barrier side of correlation diagram.

The problem with implementing a calculation based on the torsional model of Eqs. (2)–(6) is that of choosing a value for the effective rotational constant. An upper limit on this rotational constant would be 27 cm^{-1}, the *A* rota-

tional constant of water. However, because this assumes that the water subunit symmetry axis is perpendicular to the complex a axis, this would yield zero dipole along the a axis, inconsistent with experiment. The moment of inertia for water rotating about an OH bond is 0.864 amu Å^2, yielding a rotational constant of 19.5 cm^{-1}. This would be the $m=0\rightarrow\pm1$ transition energy of the complex in the absence of any barrier to torsion at all. Introducing a barrier splits the $0\rightarrow\pm1$ transition energy rapidly. Thus, if the bond were a linear hydrogen bond, with no bending, the torsional rotation of the free proton about this bond would be entirely unhindered. The absence of a barrier seems unreasonable, so this choice of rotational constant is rejected.

At the lowest extreme would be the effective rotational constant 17.2 cm^{-1} given by a geometry in which the free OH bond is perpendicular to the complex a axis. The frequency of the upper $m=0\rightarrow\pm1$ transition increases from this value, so it is conceivable that the effective rotational constant is this low. Although this geometry is not completely consistent with the dipole observed,[13] it is the only "reasonable" choice for the internal rotation constant. One can then introduce a potential $V_2=2.4$ cm^{-1}, for a barrier of 4.8 cm^{-1} before the $0\rightarrow\pm1_{\text{upper}}$ transition rises to 19.7 cm^{-1}. Since the internal rotation constant is taken to be at its lower bound, this modeling suggests that 4.8 cm^{-1} is in fact an upper bound for the barrier height. This simple calculation predicts the $0\rightarrow\pm1_{\text{lower}}$ transition at 14.8 cm^{-1}, well below the lower limit of the region scanned in this work.

V. CONCLUSIONS

We have observed and identified a torsional vibrational transition of the propane–water complex. This spectrum and the microwave spectrum presented in the accompanying paper[13] indicate that all three atoms of water are in the CCC plane of the propane, and the current data suggest there is only slight (<5 cm^{-1}) hindrance to internal rotation about the CH–O hydrogen bond. Further data are clearly needed before more complete conclusions can be drawn about the intermolecular potential energy surface.

ACKNOWLEDGMENTS

We are grateful to Dr. R. D. Suenram and Dr. F. J. Lovas for the collaboration on the microwave spectrum that, ultimately, brought this work to fruition. We further thank Dr. R. D. Suenram for help in designing and implementing the Stark modification, and Jennifer Loeser for helpful discussions regarding the group theoretical aspects of this work. This work was supported by the Experimental Physical Chemistry Program of the National Science Foundation (Grant No. CHE-9123335).

[1] L. R. Pratt and D. Chandler, J. Chem. Phys. **73**, 3434 (1980).
[2] A. Ben-Naim, *Hydrophobic Interactions* (Plenum, New York, 1980); J. Chem. Phys. **90**, 7412 (1989).
[3] J. H. van der Waals and P. C. Platteeuw, Adv. Chem. Phys. **2**, 1 (1959).
[4] P. M. Rodger, J. Chem. Phys. **94**, 6080 (1990).
[5] W. C. Swope and H. C. Andersen, J. Chem. Phys. **88**, 6548 (1984).
[6] R. C. Cohen, K. L. Busarow, K. B. Laughlin, G. A. Blake, M. Havenith, Y. T. Lee, and R. J. Saykally, J. Chem. Phys. **89**, 4494 (1988).
[7] R. C. Cohen, K. L. Busarow, Y. T. Lee, and R. J. Saykally, J. Chem. Phys. **92**, 169 (1990).
[8] R. C. Cohen and R. J. Saykally, J. Phys. Chem. **94**, 7991 (1990).
[9] R. C. Cohen and R. J. Saykally, J. Chem. Phys. **95**, 7891 (1991).
[10] R. C. Cohen and R. J. Saykally, J. Chem. Phys. **98**, 6007 (1993).
[11] L. Dore, R. C. Cohen, C. A. Schmuttenmaer, K. L. Busarow, M. J. Elrod, J. G. Loeser, and R. J. Saykally (unpublished).
[12] G. T. Fraser, R. D. Suenram, and F. J. Lovas (unpublished).
[13] D. W. Steyert, M. J. Elrod, R. J. Saykally, F. J. Lovas, and R. D. Suenram, J. Chem. Phys. **99**, 7424 (1993).
[14] S. Suzuki, P. G. Green, R. E. Bumgarner, S. Dasgupta, W. A. Goddard III, and G. A. Blake, Science **257**, 942 (1992).
[15] G. A. Blake, K. B. Laughlin, R. C. Cohen, K. L. Busarow, D.-H. Gwo, C. A. Schmuttenmaer, D. W. Steyert, and R. J. Saykally, Rev. Sci. Instrum. **62**, 1701 (1991).
[16] D. Kaur, A. M. de Souza, J. Wanna, S. A. Hammad, L. Mercorelli, and D. S. Perry, Appl. Opt. **29**, 119 (1990).
[17] C. A. Schmuttenmaer, R. C. Cohen, N. Pugliano, J. R. Heath, A. L. Cooksy, K. L. Busarow, and R. J. Saykally, Science **249**, 897 (1990).
[18] K. L. Busarow, G. A. Blake, K. B. Laughlin, R. C. Cohen, Y. T. Lee, and R. J. Saykally, J. Chem. Phys. **89**, 1268 (1989).
[19] N. G. Douglas, *Millimetre and Submillimetre Wavelength Lasers* (Springer-Verlag, Berlin, 1989).
[20] C. H. Townes and A. L. Schawlow, *Microwave Spectroscopy* (Dover, New York, 1975).
[21] D. Ray, R. L. Robinson, D.-H. Gwo, and R. J. Saykally, J. Chem. Phys. **84**, 1171 (1986).
[22] M. D. Marshall, A. Charo, H. O. Leung, and W. Klemperer, J. Chem. Phys. **83**, 4924 (1985).
[23] J. K. G. Watson, J. Chem. Phys. **46**, 1935 (1967).
[24] M. J. Elrod, J. G. Loeser, and R. J. Saykally, J. Chem. Phys. **98**, 5352 (1993).
[25] F. J. Lovas and R. D. Suenram, J. Phys. Chem. Ref. Data **18**, 1245 (1989).
[26] P. R. Bunker, *Molecular Symmetry and Spectroscopy* (Academic, San Diego, 1979).